Detection and Identification of non-cooperative UAV using a COTS mmWave Radar

YUAN HE, Tsinghua University, China
JIA ZHANG, Tsinghua University, China
RUI XI*, University of Electronic Science and Technology of China, China
XIN NA, Tsinghua University, China
YIMIAN SUN, Tsinghua University, China
BEIBEI LI, Xi'An Xingfu Lindai Construction & Investment Co.,LTD., China

Small Unmanned Aerial Vehicles (UAVs) are becoming potential threats to security-sensitive areas and personal privacy. A UAV can shoot photos at height, but how to detect such an uninvited intruder is an open problem. This paper presents mmHawkeye, a passive approach for non-cooperative UAV detection and identification with a COTS millimeter wave (mmWave) radar. mmHawkeye doesn't require prior knowledge of the type, motions, and flight trajectory of the UAV, while exploiting the signal feature induced by the UAV's periodic micro-motion (PMM) for long-range accurate detection. The design is therefore effective in dealing with low-SNR and uncertain reflected signals from the UAV. After analyzing the theoretical model of the PMM feature, mmHawkeye can further track the UAV's position containing range, azimuth and altitude angle with dynamic programming and particle filtering, and then identify it with a Long Short-Term Memory (LSTM) based detector. We implement mmHawkeye on a commercial mmWave radar and evaluate its performance under varied settings. The experimental results show that mmHawkeye has a detection accuracy of 95.8% and can realize detection at a range up to 80m.

CCS Concepts: • **Computer systems organization → Embedded and cyber-physical systems**; • **Hardware → Sensor applications and deployments**.

Additional Key Words and Phrases: Passive detection, Periodic micro-motion, LSTM, Millimeter Wave, UAV

ACM Reference Format:
Yuan He, Jia Zhang, Rui Xi, Xin Na, Yimian Sun, and Beibei Li. 2023. Detection and Identification of non-cooperative UAV using a COTS mmWave Radar. 1, 1 (December 2023), 23 pages. https://doi.org/XXXXXXX.XXXXXXX

1 INTRODUCTION

With the proliferation of small Unmanned Aerial Vehicles (UAVs), threats of UAVs arise, such as intrusion into personal space [36], illegal item delivery [6], public safety threat [30] and human

*Corresponding author.

Authors' addresses: Yuan He, heyuan@mail.tsinghua.edu.cn, Tsinghua University, 30 Shuangqing Rd, Haidian District, Beijing, China, 100084; Jia Zhang, j-zhang19@mails.tsinghua.edu.cn, Tsinghua University, 30 Shuangqing Rd, Haidian District, Beijing, China, 100084; Rui Xi, ruix.ryan@gmail.com, University of Electronic Science and Technology of China, No.2006, Xiyuan Ave, West Hi-Tech Zone, Chengdu, Sichuan, China, 611731; Xin Na, nx20@mails.tsinghua.edu.cn, Tsinghua University, 30 Shuangqing Rd, Haidian District, Beijing, China, 100084; Yimian Sun, sym21@mails.tsinghua.edu.cn, Tsinghua University, 30 Shuangqing Rd, Haidian District, Beijing, China, 100084; Beibei Li, libeibei1@cscec.com, Xi'An Xingfu Lindai Construction & Investment Co.,LTD., Hansen Rd, Xincheng District, XI'AN, China, 710000.

XXXX-XXXX/2023/12-ART $15.00
https://doi.org/XXXXXXX.XXXXXXX

injury [2], etc. Uninvited intrusion into personal space is most widely concerned, as it threats the privacy and safety of individuals. Without mandatory restrictions, a UAV can easily but illegally intrude personal space at height to conduct activities such as candid photography or even theft. Since such UAVs are often very small and hard to spot with the naked eye, how to detect them becomes an extremely important and urgent problem.

A UAV detection system is desired to meet multiple goals: First, the detection approach should be passive, i.e., the detection process shouldn't require the cooperation of the UAV. Second, the system should be able to detect the presence of a UAV at height. Third, the detection system should be low-cost and easy to deploy, considering potentially a large population of ordinary users. Last but not least, the system should be generic to detect a variety of UAVs in various illumination and noise conditions.

Unfortunately, we find limitations in the existing approaches for UAV detection. Specifically, sound-based UAV detection [39, 43] is easily interfered by complex environmental noise. The sound of UAV attenuates fast in the air, so sound-based approaches generally have a limited detection range. Their performance further degrades when the UAV employs the noise reduction technique. Vision-based UAV detection [8, 57] can work when the UAV is visible, but its accuracy and reliability are susceptible to illumination conditions and visual background. Thermal and Infrared Radiation (IR) imaging cameras [1] are possible options, but they are expensive and have limited coverage. There are also proposals of UAV detection based on RF signals [5, 16, 32, 33], which need to use special instruments to capture and analyze the communication of non-cooperative UAVs. Traditional radars [25] are too expensive and power-consuming. In short, none of the existing approaches is suitable for UAV detection in daily usage scenarios.

Specifically, non-cooperative UAV detection faces the following challenges: Firstly, the small size of the UAV makes the reflected signal very weak and easily overwhelmed by environmental noise. Secondly, Detecting the UAV at height requires the detection system to cover a large detection range. Thirdly, the unknown information of the non-cooperative UAVs (e.g., model, size, etc.) makes accurate UAV detection more challenging. Finally, as the daily scenarios are very complex, the UAV should be detected in various illumination and noise conditions.

In this paper, we explore the feasibility of using a COTS (Commercial-Off-the-shelf) mmWave (millimeter Wave) radar for UAV detection. mmWave radar-based sensing [9, 24, 50, 53, 55] has attracted a large body of research in the last few years. The UAV-reflected signals received by the radar contain rich information associated with the UAV. But it is a daunting task to accurately detect and identify a UAV from such signals, due to the following reasons: First, since a COTS radar has limited transmission power and the UAV is usually small and at height from the radar, the signals reflected from the UAV and received by the radar are very weak. This problem is particularly common in intrusion into personal space, as the small UAVs tend to conduct candid photography at height. Conventional approaches based on the signal intensity for target detection [3, 10, 18, 19, 31, 51, 58] become ineffective in such contexts. Second, the motions of a non-cooperative UAV (e.g., turning and hovering, etc.) are dynamic and unpredictable, making it extremely difficult to extract the UAV-reflected signals from the received signals. The intruders often temporarily adjust their flight trajectories based on their targets, making the UAV's motions unpredictable. Third, the UAV-reflected signals contain both the inherent features of the UAV and the motion-related features, which are tightly coupled with one another. The motion-related features can confuse the intruding UAVs with other objects such as birds, resulting in a high false alarm rate. The above factors collectively lead to the very low signal-to-noise ratio (SNR) and the uncertainty of the UAV-reflected signals.

To address the above challenges, we try to exploit a unique signal feature that can help us to extract and identify the reflected signals of the UAV. This feature is desired to be motion-independent, stable over time, consistent across different types of UAVs, and distinguishable from noise. Our

finding is that the periodic micro-motion (PMM) of the UAV (such as propeller rotation, etc.) can be converted into stable and consistent features of the frequency of the reflected mmWave signals. Specifically, the periodic micro-motion always induces periodic frequency modulation of the reflected signal, resulting in a series of periodic peaks in the frequency spectrum. Based on this finding, we propose mmHawkeye, a PMM-based UAV passive detection approach with a COTS mmWave radar. mmHawkeye first extracts and enhances the periodic features with spectrum folding technology to enhance the signal SNR. To deal with unpredictable UAV motions, a novel tracking algorithm incorporating dynamic programming and particle filtering, is designed to obtain the UAV's location containing range (r), azimuth angle (θ) and altitude angle (φ). Given a sequence of UAV's locations, mmHawkeye extracts the corresponding Dopper spectrums to form a Dopper-time-diagram, which is then fed into an LSTM-based detector for accurate UAV identification.

Our contributions can be summarized as follows:

• To the best of our knowledge, mmHawkeye is the first mmWave-based long-range UAV detection approach. By exploiting the reflected signal features from the UAV, mmHawkeye is able to detect and identify an uncooperative UAV with very weak signals.

• We propose tailored algorithms based on the PMM feature to fully utilize the reflected signal from the UAV, including feature extraction based on feature periodicity, UAV tracking with trajectory continuity and motion-independent UAV identification.

• We implement mmHawkeye on the commercial radar (TI IWR6843ISKODS board) and conduct extensive experiments. The results demonstrate that mmHawkeye achieves an average UAV detection accuracy of 95.8% and an average relative range error of 0.9% at a detection range up to 80m. To the best of our knowledge, mmHawkeye is the first work to detect small UAVs at such a long range using only a COTS mmWave radar.

The rest of the paper is organized as follows. Section 2 presents the sensing model and the PMM feature, which are the theoretical foundation of this work. Section 3 elaborates on the design of mmHawkeye. The implementation details and evaluation results are presented in Section 4. Section 5 discusses practical issues and future work. Section 6 reviews the related work. Section 7 concludes this work.

2 THEORETICAL MODEL

In this section, we first introduce the theoretical model of the PMM feature, which theoretically exists stably during the UAV flight. Then we conduct some preliminary studies to verify the stability of the PMM feature and demonstrate the feasibility of UAV detection and tracking with the PMM feature.

2.1 The Sensing Model and the PMM Feature

As shown in Fig. 1, the mmWave radar is deployed on the ground and faces upward and sends *frequency-modulated continuous wave* (FMCW) chirp signals. When a small UAV is flying across the radar's sensing area, the emitted signals hit the UAV and reflect back to the radar. Due to its radial motion relative to the radar, the flying UAV will induce a certain frequency modulation of the reflected signal, which appears as a spectral shift peak in the Doppler spectrum of the reflected mmWave signal, called the body velocity peak. Meanwhile, the components of the flying UAV (such as rotating blades) have additional periodic micro-motions. These periodic micro-motions will induce the additional periodic and time-varying frequency modulation of the reflected signal, which causes a series of periodic peaks in the Doppler spectrum centered on the body velocity peak.

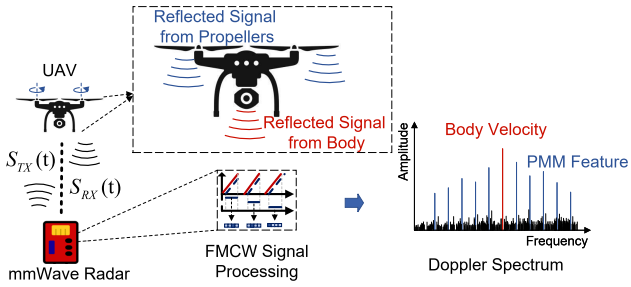

Fig. 1. The sensing model

Specifically, a mmWave radar sends chirp signals for range estimation and velocity measurement. The frequency difference between the transmitted signal (Tx) and the received signal (Rx) indicates the signal propagation time, which can be used to calculate the distance of the target. Denoting the time-variant distance between the radar and the target by $R(t)$, the transmitted signal and the received signal can be expressed as:

$$\begin{aligned} S_{Tx}(t) &= exp[j(2\pi f_c t + \pi K t^2)] \\ S_{Rx}(t) &= \alpha S_{Tx}[t - 2R(t)/c] \end{aligned} \tag{1}$$

where f_c and K represent the starting frequency and the chirp slope of the FMCW signal, respectively. α is the propagation loss. By mixing the transmitted signal and the received signal, the *beat frequency signal* $s(t)$ can be obtained as:

$$s_{bf}(t) = S^*_{Tx}(t)S_{Rx}(t) = \alpha exp[j4\pi(f_c + Kt)R(t)/c] \tag{2}$$

whose phase value indicates the distance $R(t)$.

To obtain the range and the radial velocity of the target, we first conduct a *Range-FFT* operation [17] on the samples of $s_{bf}(t)$ during a chirp. In this way, the frequency spectrum of $s_{bf}(t)$ is mapped to the range spectrum and the distance of the target can be obtained.

Since the duration of a chirp is around 0.5ms, we can neglect the displacement during this period and focus on the distance change across consecutive chirps. By combining the samples in a certain bin from the Range-FFT results, we can obtain the reflected signal $S(t)$ from the target range bin:

$$S(t) = \alpha exp[j4\pi f_c R(t)/c] \tag{3}$$

If the distance $R(t)$ can be rewritten as $R(t) = R_0 + vt$, R_0 and v are the current distance and the radial velocity, respectively. We then perform a *Doppler-FFT* operation [17] on the samples of $S(t)$ to obtain the Doppler spectrum:

$$S(f) = \alpha\delta(f - 2vf_c/c) \tag{4}$$

where $\delta()$ is the Dirac delta function. The peak of the Doppler spectrum indicates the target velocity. With Range-Doppler-FFT, we can obtain the Range-Doppler spectrum and estimate the range and the velocity of the target.

When the detection target is a UAV, we need to consider not only the body motion of the UAV, but also the impact of these components with periodic micro-motion on the reflected signal. The theoretical model is shown in Fig. 2. To simplify the understanding, we assume that the UAV's radial velocity relative to the mmWave radar is v and the rotational angular velocity of each blade is w. Similarly, considering the small size of the UAV and the long distance between UAV and radar, we also assume that the rotors all exist in a certain range bin and the number of rotors is Q. The

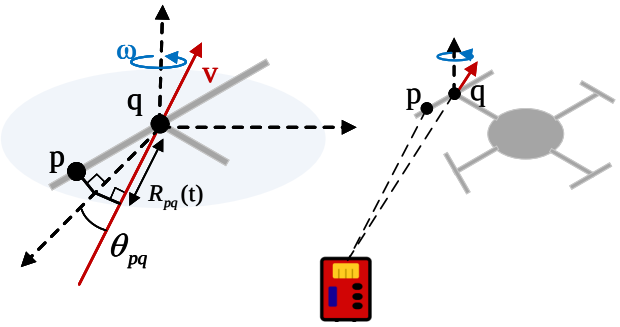

Fig. 2. The theoretical model of the PMM feature

blades of each rotor can be viewed as consisting of P scattering points. Then we derive the impact of the periodic micro-motion of the blades on the reflected signal.

Firstly, considering that the distance between UAV and radar is much larger than the distance from the scattering point to the rotor, the distance between the p-th scattering point in the q-th blade and the mmWave radar $R_p(t)$ can be represented as:

$$\begin{aligned} R_p(t) &= R_q(t) + R_{pq}(t) \\ R_q(t) &= R_q + vt \\ R_{pq}(t) &= r_{pq} * cos(\theta_{pq}) * cos(\omega t + \phi_{pq}) \end{aligned} \tag{5}$$

where $R_q(t)$ represents the distance between the q-th rotor and the mmWave radar, R_q is its current distance. the distance between the p-th scatter point and the rotor is represented as r_{pq} and its projection to the velocity direction is represented $R_{pq}(t)$. θ_{pq} is the angle between the blade plane and the velocity direction, and ϕ_{pq} is the rotation initial phase of the p-th scattering point.

We can find that both the radial velocity of the UAV and the blade rotation angular velocity affect the distance between the scattering point and the mmWave radar, which in turn affects the reflected signal. The reflected signal from the scatter point can be expressed as:

$$S_{pq}(t) = \beta_{pq} exp\{j4\pi f_c[R_q(t) + R_{pq}(t)]/c\} \tag{6}$$

where β_{pq} represents the propagation loss, which is related to the propagation distance, the material and roughness of the scattering point, etc. By adding the reflected signals from all scatter points and the body together, we can obtain the reflected signal of a flying UAV:

$$\begin{aligned} S(t) =& \alpha exp[j4\pi f_c R(t)/c] + \\ & \sum_{q=1}^{Q}\sum_{p=1}^{P} \beta_{pq} exp\{j4\pi f_c[R_q(t) + R_{pq}(t)]/c\} \end{aligned} \tag{7}$$

If we perform a Doppler-FFT operation on this reflected signal, its Doppler spectrum can be represented as:

$$\begin{aligned} S(f) =& \alpha\delta(f - 2vf_c/c) + \\ & \sum_{q=1}^{Q}\sum_{p=1}^{P}\sum_{m=-\infty}^{+\infty} \gamma_{pq}\delta(f - 2vf_c/c - \omega m/2\pi) \end{aligned} \tag{8}$$

where γ_{pqm} denotes the m-th frequency loss of a scattering point, which is a complex function of m, β_{pq}, r_{pq}, ϕ_{pq} and θ_{pq}. For more calculation details, the reader can refer to the related work [22].

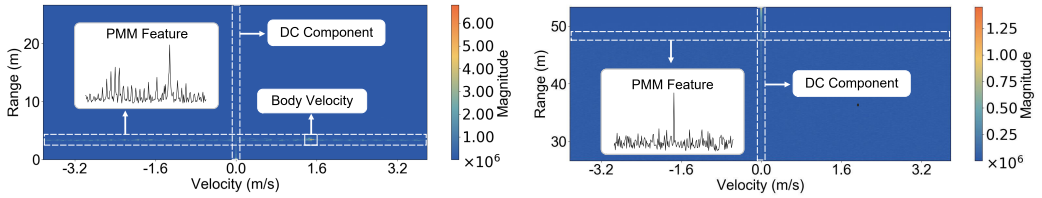

(a) The ascending UAV (b) The hovering UAV

Fig. 3. The Range-Doppler spectrum of the UAV

This formula shows that there will be a series of periodic peaks centered on the body velocity peak in the Doppler spectrum. We call these peaks **the PMM feature**:

$$\begin{cases} \text{Peak Pos} : 2vf_c/c + \omega m/2\pi & m \in Z \\ \text{Peak value} : \sum_{q=1}^{Q} \sum_{p=1}^{P} \gamma_{pqm} & m \in Z \end{cases} \tag{9}$$

The interval between the peaks is the same ($\omega/2\pi$) and is determined by the propeller rotation velocity. The peak values are more complex and related to the UAV relative position (β_{pq}, θ_{pq}) and the UAV structure (r_{pq}, ϕ_{pq}, P, Q).

With the derivation of the PMM feature, we can find that the PMM feature exists stably during the UAV's flight. The structure and position of a UAV only affect the peak values rather than the peak intervals. This means that the number of propellers, the number of blades and the blade length don't affect the peak intervals. Such a stable feature can be used to detect various UAVs. Without loss of generality, we use a six-wing UAV as an example in later sections.

2.2 PMM in Reality

We give the observations on PMM to demonstrate the feasibility of UAV detection with the PMM feature.

In our experiments, a commercial mmWave radar (TI IWR6843ISKODS board) [14] is deployed on the ground and faces upward. A six-wing UAV with three blades per propeller is steered above the mmWave radar. The UAV is first controlled to ascend at a constant speed of about 1.5m/s and then hover at a range of 48m. We respectively select a segment of the reflected signal from these two stages and perform Range-Doppler-FFT on them. Fig. 3(a) and Fig. 3(b) show the Range-Doppler spectrum of the ascending UAV and that of the hovering UAV, respectively. The results show that: (1) Whether the UAV is moving or hovering, the PMM feature always stably appears in the range bin where the UAV is located. In contrast, the reflection intensity and the radial velocity features are less stable as they are more easily affected by the relative distance and the UAV's motions. (2) When the distance between UAV and radar is far, the PMM feature shrinks and distorts, due to the degraded quality of the reflected signal. Nevertheless, its periodicity still exists stably. Note that the highest peak of the PMM feature in Fig. 3(b) corresponds to the Direct Current (DC) components. In this case, we try to exploit the periodicity of the UAV's PMM feature to extract and identify the reflected signal of the UAV.

3 MMHAWKEYE DESIGN

This section starts with an overview of mmHawkeye, and then introduces three key modules of the design respectively.

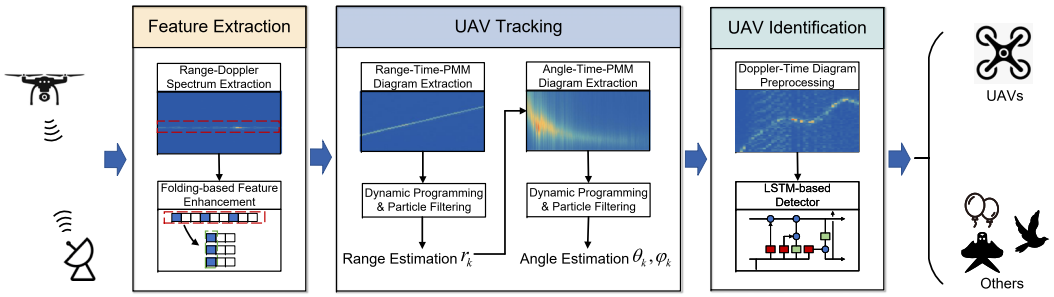

Fig. 4. The overflow of mmHawkeye

3.1 Overview

mmHawkeye solves the UAV detection problem in three steps, which correspond to the three key modules in its design, namely feature extraction, UAV tracking and UAV identification. Fig. 4 shows the overview of mmHawkeye.

• *Feature extraction.* mmHawkeye continuously extracts the Range-Doppler spectrums with Range-Doppler-FFT. To distinguish the PMM feature from the environment noise in each Range-Doppler spectrum, We perform spectrum folding on each Doppler spectrum. If the PMM feature exists, it will be significantly enhanced by spectrum folding and the folding result can be used for further tracking and detection.

• *UAV tracking.* With feature extraction, mmHawkeye continuously extracts the folding results in Range-Doppler spectrums, which collectively form the Range-Time-PMM diagram. To cope with the impact of unpredictable UAV motions, we design a tracking algorithm based on dynamic programming and particle filtering to obtain the range results from the Range-Time-PMM diagram. Furthermore, as UAV's distance is known, mmHawkeye applies a beamforming technique to obtain the Angle-Doppler spectrum, and then estimates the UAV's angles using similar operations to range estimation.

• *UAV identification.* After obtaining the target's tracking result, mmHawkeye continuously extracts the Doppler spectrums from the target's location, forming the Doppler-Time diagram. After preprocessing the diagram via DC removal and feature alignment, the Doppler-Time segments are fed into an LSTM-based detector for UAV identification.

3.2 Feature Extraction

The feature extraction module employs the spectrum folding technique to amplify the difference between the PMM feature and the environment noise. Below is the detail of this module.

As we mentioned before, we can obtain the Range-Doppler spectrum by performing Range-Doppler-FFT on the reflected mmWave signals. Specifically, we use $\{D_1, D_2, ..., D_R\}$ to represent the Doppler spectrums in a Range-Doppler spectrum. D_i and R represent the Doppler spectrum in the i-th range bin and the number of range bins, respectively. The number of Doppler bins in a Doppler spectrum is L. When the UAV appears in the i-th range bin, the PMM feature will appear in the corresponding Doppler spectrum D_i. However, considering the unpredictable propeller rotation velocity, the period of the peaks in the PMM feature is uncertain and variable. Those periodic peaks may even be buried in environment noise due to the low SNR of the reflected signal.

We employ the folding technique [26] to extract and enhance the PMM feature, which is used to find signal periodicity under noise. An example of the folding process is shown in Fig. 5, where the values of Doppler bins are represented by boxes. The black boxes represent the periodic peaks in

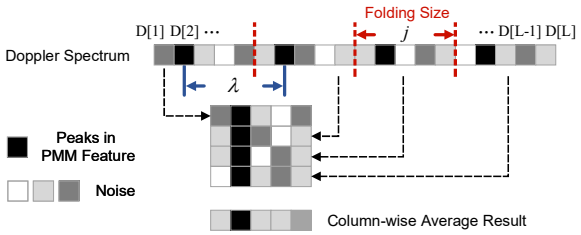

Fig. 5. The folding process of the PMM feature

the PMM feature and the other boxes represent the noise. The interval λ between adjacent peaks in the Doppler spectrum is 5 and the number of Doppler bins L is 20. If we exactly fold the Doppler spectrum into a matrix with $j = \lambda$ columns, the periodic peaks will align in a column and there will be a significantly enhanced peak in the column-wise averaged result. For clarity, the maximum value in the column-wise averaged result and the number of folding columns are referred to as the folding value and the folding size, respectively. When the folding size j is not equal to λ, the folding value will decrease rapidly as the peaks are not aligned.

Note that the interval between adjacent peaks in the PMM feature is determined by the propeller rotation velocity, it is unpredictable and may change at any time. To find the right folding size, we traverse all integers in an empirical range $[j_{min}, j_{max}]$ and calculate the corresponding folding values, where j_{min} and j_{max} represent the minimum and maximum folding size, respectively. They are set to 2 and 20 according to the propeller rotation velocity range and the Doppler spectrum resolution. With the fixed traversing range, the computation time can be controlled. The folding value of Doppler spectrum D_i with folding size j can be calculated by:

$$F_i(j) = \max_{1 \le k \le j} \frac{\sum_{1 \le m \le M} D_i[k + (m-1) * j]}{M} \tag{10}$$

where k and m denote the folding column index and the row index in the folding matrix, respectively. The number of rows in the folding matrix is represented by M, which can be calculated by $M = \lfloor \frac{L}{j} \rfloor$.

The largest folding value is selected to be the folding result, which increases significantly when the PMM feature exists. The folding result of the Doppler spectrum D_i can be calculated by:

$$P_i = \max_{j_{min} \le j \le j_{max}} F_i(j) \tag{11}$$

In this way, mmHawkeye can calculate the folding result of each Doppler spectrum. Since the PMM feature of the UAV has a stable periodicity, its folding result is much larger than that of the random environment noise. These folding results can be further used for UAV tracking and detection.

3.3 UAV Tracking

The UAV tracking module first preprocesses the folding results with spectral subtraction, so that the impact of the static background noise is mitigated. Then the UAV tracking is realized through dynamic programming and particle filtering, where the unpredictable UAV motions and the local dynamic noise are taken into account and appropriately dealt with.

To estimate the UAV trajectory, mmHawkeye continuously extracts the folding results with feature extraction. These folding results form a Range-Time-PMM diagram, denoted by the R-PMM. Suppose that there are T Range-Doppler spectrums and each Range-Doppler spectrum has R range

bins, the value of R-PMM(r, t) represents the folding result of the r-th range bin in the t-th Range-Doppler spectrum. As the Doppler spectrum of the UAV has a larger folding result at each moment, the UAV trajectory corresponds to a series of range bins that contain larger values in the R-PMM. These range bins can form a maximum path in the R-PMM whose cumulative folding result over time is the maximum among all paths. Therefore, we can track the UAV by searching for the maximum path in the R-PMM.

Considering that the intensity of the Doppler spectrum is proportional to the reflected signal intensity, there are different static background noise intensities in different range bins in the R-PMM. To mitigate the impact of such noise, we employ the spectral subtraction algorithm [42] to preprocess the R-PMM. The main idea is to subtract the estimation of the average background noise spectrum from the noisy R-PMM. Specifically, the average background noise spectrum can be estimated by:

$$N(r) = \frac{1}{T}\sum_{t=1}^{T} N(r,t) \tag{12}$$

where $N(r,t)$ is the R-PMM measured in the background noise. The gain of the background noise is calculated as a normalized projection of the noisy R-PMM onto the background noise spectrum:

$$G(t) = \sum_{r=1}^{R} \frac{N(r)S(r,t)}{||N||^2} \tag{13}$$

where $S(r,t)$ is the measured R-PMM in the tracking phase and $||N|| = \sqrt{N(1)^2 + N(2)^2 + ... + N(R)^2}$ is the Euclidean norm of the noise spectrum. Finally, the background noise can be removed from the measured R-PMM as follows:

$$S^{'}(r,t) = S(r,t) - G(t)N(r) \tag{14}$$

In this way, the range-related static background noise can be removed and the preprocessed R-PMM can be used to find the maximum path, which corresponds to the UAV tracking result. The maximum path g^* can be obtained by solving:

$$g^* = \arg\max_{g}\left(\sum_{t=1}^{T} S^{'}(g(t),t)\right) \tag{15}$$

where $g = (t, g(t))_{t=1}^{T}$ is denoted as a path.

However, since the folding result characterizes the PMM feature of the UAV, it may change rapidly due to unpredictable UAV motions. On the other hand, impacted by the complex environment and imperfect hardware, there may still be local dynamic noise in the vicinity of the UAV trajectory in the R-PMM. Both of them lead to degradation in tracking accuracy.

Considering that the UAV trajectory always changes continuously, mmHawkeye utilizes the trajectory continuity to reduce the tracking errors. Specifically, assume that the maximum flight speed of the UAV is V_{max} and the duration of the Range-Doppler spectrum is T_d, the maximum range bin variation of the UAV in the adjacent columns of the R-PMM can be calculated by:

$$K = \lceil \frac{V_{max} * T_d}{R_{res}} \rceil \tag{16}$$

where R_{res} represents the range resolution of the mmWave radar. The path in the R-PMM corresponding to the UAV trajectory always satisfies this constraint. Therefore, the UAV tracking problem can be further transformed into the problem of finding a constrained maximum path in the

R-PMM, where the variation of adjacent columns in the path does not exceed K. This constrained maximum path can be found by solving:

$$\begin{aligned} g^* &= \arg\max_{g}(\sum_{t=1}^{T} S^{'}(g(t),t)) \\ s.t.\ &|g(t)-g(t-1)| \leq K \end{aligned} \tag{17}$$

This problem can be solved by dynamic programming. Specifically, we first define the score at bin (r,t) as the constrained maximum cumulative folding result, which can be calculated as:

$$\theta(r,t) = \max_{k\in[-K,K]} \theta(r+k,t-1) + S^{'}(r,t) \tag{18}$$

Since $\theta(r,t)$ considers both the trajectory continuity and the previous cumulative folding results, its calculation process obtains the constrained optimal track through the bin (r,t). To obtain the entire constrained maximum path, we first find the bin $(T, g^*(T))$ in the last column that contributes to the maximum score. Then the rest of the path can be obtained by:

$$\begin{aligned} g^*(t) &= \arg\max_{k\in[-K,K]} \theta(g^*(t+1)+k,t) + g^*(t+1) \\ \forall\ t &= T-1, T-2, ..., 1 \end{aligned} \tag{19}$$

This backtracking procedure provides the constrained maximum path g^*, which is the optimal solution for Eq. 17. In this way, we can obtain the UAV tracking result.

mmHawkeye further applies the particle filter [4] to the tracking result to reduce the tracking error. The particle filter can estimate the target state by combining the observation and the prediction. Specifically, the state in our particle filter includes the range and the velocity of the UAV, and the observation is the tracking result. We initialize 5000 particles with uniform distribution and use the multinomial resampling algorithm as the particle resampling method.

We further provide the users with the UAV angle estimation results. Due to the limited number of the mmWave radar's antennas, the angular resolution is limited and the angle estimation results fluctuate. However, since we can obtain accurate range estimation results, the angle estimation error can be bounded.

To obtain the angle estimation results, we first select these reflected signals of all antennas corresponding to the UAV as the UAV-related signals. Then we apply the Capon beamforming algorithm [28] to these UAV-related signals in each frame to obtain the reflected signals from each angle.

After the reflected signals from each angle are obtained, the Doppler-FFT operation can be applied to them to obtain the Angle-Doppler spectrum. The PMM feature can be captured from the angle bin where the UAV locate with the same feature extraction operation mentioned in Sec. 3.2,

These folding results from the angle bins can form an Angle-Time-PMM diagram, denoted by the A-PMM. The angle estimation results can be obtained from the A-PMM using the same operation as these of R-PMM, including spectrum subtraction, dynamic programming-based tracking and particle filter.

3.4 UAV Identification

Now we show how to utilize the PMM features to identify a UAV. We first extract the target's Doppler spectrums from a series of Range-Doppler spectrums according to the tracking result. Then the Doppler spectrums are fed into an LSTM-based) detector for UAV identification. The process of UAV identification is shown in Fig. 6.

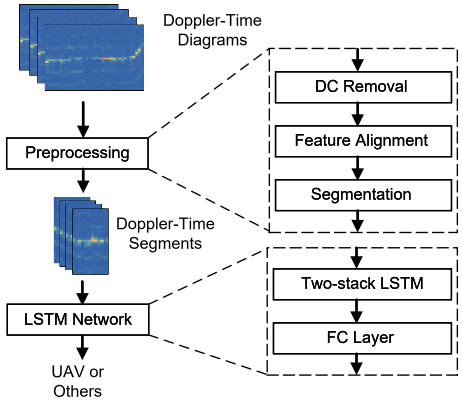

Fig. 6. The process of UAV identification

With the tracking result and the Range-Doppler spectrums, we can extract a series of Doppler spectrums from where the target is located, forming a Doppler-Time diagram. When the target is a UAV, this diagram will contain unique and continuous PMM features which can be used to distinguish the UAV from other objects.

We first remove the DC noise from the Doppler-Time diagram. Considering that the body velocity of the UAV is close to zero when it hovers, the corresponding DC component contains the body velocity peak. To preserve the body velocity peak, we average the DC components of the Doppler spectrums where the body velocity peak is not close to the DC component. Then the average value is subtracted across all the DC components. Besides, the unpredictable body velocity determines the center of the PMM feature and prevents us from exploiting the periodicity of the PMM feature. Therefore We devise a feature alignment algorithm on the Doppler-Time diagram to align each PMM feature center to the Doppler spectrum center. When the body velocity peak of the Doppler spectrum is not in the DC bin, we shift the entire Doppler spectrum along the direction from the body velocity peak to the DC bin and complement it by linear interpolation.

The preprocessed Doppler-Time diagram contains the PMM features. However, the tracking result may have errors, especially when the UAV is at height. It is not always reliable to directly use the obtained Doppler-Time diagram. To reduce the impact of tracking errors, we first split the Doppler-Time diagram into fixed-length segments. Then we compare the maximum folding result of each segment with an empirical threshold. When the maximum folding result is less than the threshold, we consider that the segment does not contain PMM features and discard it. The threshold is set to 30000 according to our extensive empirical experiments.

Finally, the preprocessed Doppler-Time segments are used to identify the UAV from other objects. Considering that when there are objects such as birds or balloons in the vicinity of the radar, their Doppler-Time segments may have high folding results and uncertain folding sizes due to the environmental noise, the simple classification methods based on statistical features of PMM, such as peak interval, mean value, etc., may be easily disturbed by such segments and severely degrade. Therefore, we design an LSTM-based detector to solve such a binary classification problem. The LSTM network [12] is a classic recurrent neural network that is suitable to process the sequences of data and has excellent performance on recognition tasks. Considering that each time slot in the Doppler-Time diagram contains L Doppler bins, the input dimension of our LSTM network is set to L. Our network contains two stacked LSTM layers and the hidden state size is set to 128. A fully connected layer is used to map the hidden state to the identification results, i.e., UAVs or other

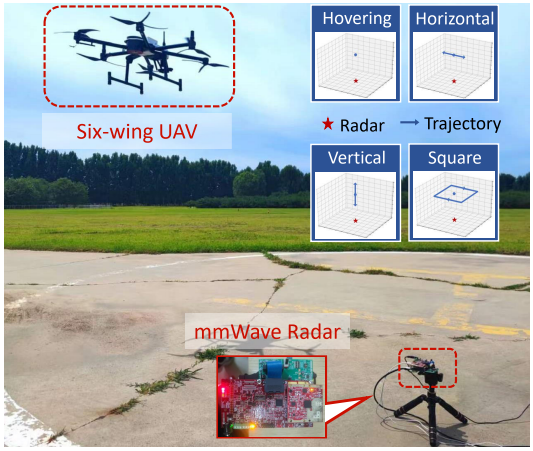

Fig. 7. The experiment scenario

objects. We select the cross entropy loss function to train our network. Considering that the peak intervals in PMM features are not affected by UAV types, our network can detect various UAVs with small training data.

4 IMPLEMENTATION AND EVALUATION

In this section, we introduce the implementation of mmHawkeye and evaluate the performance of our prototype under different settings.

4.1 Implementation

We implement mmHawkeye on a commercial mmWave radar Texas Instruments IWR6843ISKODS [14]. There are 3 Tx antennas and 2*2 Rx antennas on the radar board. In our implementation, we let three TX antennas take turns transmitting FMCW signals starting at 60.25GHz with 1.92GHz bandwidth, and all Rx antennas receive the reflected signals. The duration of a single chirp is 900us and each frame includes 100 chirps. The frequency slope of the FMCW signal is 9.994MHz/us and the ADC sample rate is 6250kHz. So the radar's maximum sensing range can reach $\frac{3\times10^8 m/s\times6250kHz}{9.994MHz/us\times2} = 93.8m$. The angle of the radar's field of view (FoV) is about 120°, which is large enough to cover the experimental scene. The ADC samples from the radar are captured by a Ti DCA1000EVM data acquisition board [13] and then transmitted to a computer with an Intel Core i9-11900H 2.5GHz CPU for processing.

The experiment scenario is shown in Fig. 7. The radar is fixed horizontally on a tripod mount and is calibrated with a corner reflector in advance. A six-wing UAV with three blades per propeller is used as the detection target. The UAV weights about 8kg and each blade is about 25cm long. It has a maximum velocity of 4m/s. The UAV is equipped with a Real-time Kinematic Positioning (RTK) module [45] to provide the ground truth of the UAV's location, which has a cm-level precision. We collect the reflected signals of the UAV from different flight trajectories, at different altitudes and different velocities. These reflected signals are first processed to obtain the tracking results and the corresponding Doppler-Time diagrams. The tracking results are aligned with the ground truth by their timestamps and trajectory features. Then the Doppler-Time diagrams are split into segments of 3.6s duration. We collect more than 4000 seconds of signals under different settings and generate over 1000 segments. We further generate the same amount of the other objects' segments

by recording the Doppler-Time diagrams of kites, birds, balloons and shaking trees. We place the radar under balloons, kites, and shaking trees for data collection, and near a nest for bird data collection. These two types of segments together form our dataset. In our implementation, we use the random 70% of the segments as the training set and the rest 30% as the test set. The model is trained using the Adam optimizer with a learning rate of 0.00005 and a batch size of 10.

4.2 Methodology

We use *accuracy*, *precision*, *recall* and F1-*score* as the performance metrics to evaluate the performance of mmHawkeye. The accuracy, precision, recall and F1-score are calculated from True Positive (TP), True Negative (TN), False Positive (FP) and False Negative (FN). They are calculated as follows: $accuracy = \frac{TP+TN}{TP+FP+FN+TN}$, $precision = \frac{TP}{TP+FP}$, $recall = \frac{TP}{TP+FN}$ and $F1\text{-}score = \frac{2*precision*recall}{precision+recall}$.

To clearly show the whole detection process, we also evaluate the UAV tracking performance. We measure the tracking accuracy with the average relative range error. It calculates as follows:

$$\frac{1}{N}\sum_{n=1}^{N}\frac{|G(n)-T(n)|}{G(n)} \tag{20}$$

where $G(n)$ and $T(n)$ represent the actual range and the tracking range at the n-th sampling timestamp, respectively. N is the number of the sampling timestamps in a trace.

4.3 Overall Performance

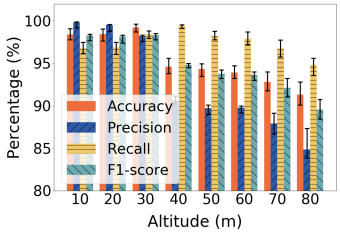

Fig. 8. The overall performance of UAV detection

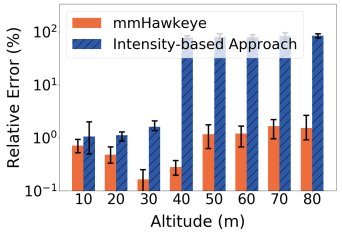

Fig. 9. The overall performance of UAV tracking

4.3.1 Detection accuracy. We first evaluate the overall detection performance of mmHawkeye. The UAV is controlled to perform different flight trajectories. The flight altitude varies from 10m to 80m. The flight trajectories at each altitude include hovering, horizontal flight, vertical flight and flying with a horizontal square. The radar is placed on the ground and vertically aligned with the horizontal center of the trajectories. The detection results at different altitudes are shown in Fig. 8. The overall detection accuracy of mmHawkeye is 95.8% (corresponding with 92.6% of precision, 97.2% of recall and 94.8% of F1-score). With the UAV altitude increasing, the detection accuracy decreases from 98.3% to 91.3%. When the UAV altitude is 10m, mmHawkeye achieves an accuracy up to 98.3%, a precision of 99.8%, a recall of 96.8% and a F1-score of 98.3%. When the altitude increases to 80m, the detection performance falls to an accuracy of 91.3%, a precision of 84.8%, a recall of 94.8% and a F1-score of 89.5%. As the UAV altitude increases, the PMM feature extracted from the received signal becomes weaker and sometimes incomplete, which leads to degradation in the detection performance. mmHawkeye keeps a high recall, which means that it can effectively detect most of the UAVs even when the UAVs are at height.

Furthermore, we verify the effectiveness of the LSTM network, using Convolutional Neural Network (CNN) to replace LSTM for binary classification. Similar to the LSTM detector in this work, only two layers of 2D CNN are used and the extracted feature are of the same size to ensure the fairness of the comparison as much as possible. The overall detection accuracy is only 68.67% (corresponding with 68.47% of precision, 99.76% of recall and 81.21% of F1-score). This is because the CNN network is only capable of obtaining local area features, but has insufficient performance in long-term data.

In addition, we calculate the Receiver Operating Characteristic (ROC) curve and the Area Under Curve (AUC) of the two network models to evaluate their performance. The ROC curve can easily detect the impact of any threshold on the generalization performance of the learner. AUC is defined as the area enclosed by the ROC curve and the coordinate axis. The closer the value is to 1.0, the higher the authenticity of the detection method. From the results shown in Fig. 10 and 11, we can find that the AUC value of mmHawkeye is higher than 0.9, which is much better than that of the variant with CNN. It means that mmHawkeye has good generalization and good stability in practical applications. As all we know, there are also a large number of network models whose performance is much better than the LSTM designed in this paper. However, it is out of the scope of this work, we prefer to leave it in the practical applications.

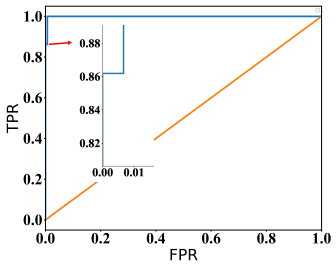

Fig. 10. The ROC curve and AUC of mmHawkeye

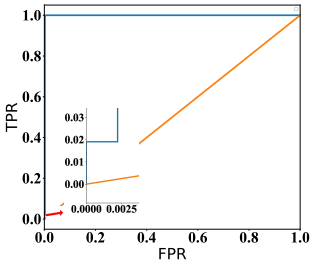

Fig. 11. The ROC curve and AUC of the variant with CNN

We also evaluate the detection efficiency. Since our network is lightweight, it only takes about 0.17s to obtain the detection results, as shown in TABLE 1. This means that mmHawkeye can provide almost real-time detection capabilities once the target is tracked.

4.3.2 Tracking accuracy. We further evaluate the tracking performance. We compare mmHawkeye with the intensity-based tracking approach commonly used in previous works such as WaveEar [49] and mmTrack [46], which select the largest value of the Range-FFT result as the tracking result. For consistency and fairness, we also perform preprocessing, dynamic programming, and particle filtering on the result of the compared approach. The tracking results of mmHawkeye at different altitudes are shown in Fig. 9. The results show that mmHawkeye can achieve a detection range of 80m, which is much higher than the detection range of 30m with the intensity-based approach. When the UAV altitude is below 30m, our tracking algorithm can achieve a more accurate range estimation compared with the intensity-based approach. The average relative range error of mmHawkeye decreases as the altitude increases. The reason is that the average range error of mmHawkeye remains less than 10cm within 30m, resulting in a reduction in average relative tracing error. When the UAV altitude is above 30m, the intensity-based approach fails completely due to the low SNR of the reflected signal. In comparison, mmHawkeye keeps accurate and has less than 2% relative range error within 80m. This is mainly attributed to the utilization the UAV's PMM feature, which helps to efficiently distinguish UAVs from the environment noise.

4.4 The Impact of Different Factors

4.4.1 The impact of the UAV's trajectory. In this experiment, We evaluate the detection performance under different trajectories of the UAV. The results are shown in Fig. 12. The detection accuracy varies slightly from 95.3% to 96.6% across different types of trajectories. Since the micro-motion of the UAV's propellers always exists in different trajectories, the PMM feature remains consistent and can be used to resist the impact of the unpredictable UAV's motion and in turn keeps the good detection performance.

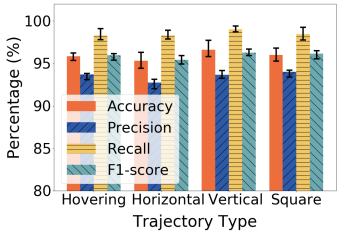

Fig. 12. The impact of UAV trajectory on detection results

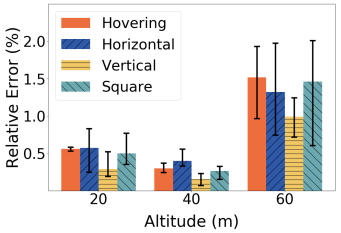

Fig. 13. The impact of UAV trajectory on tracking results

We also evaluate the tracking performance under different trajectories of the UAV. The average relative range errors under different trajectories at three altitudes (20m, 40m, 60m) are shown in Fig. 13. The range errors vary slightly with the types of UAV trajectory at each altitude and the range errors with the vertical flight are the lowest. The reason is that when the UAV is flying vertically, its radial velocity is the largest and the calculated folding result is more distinguishable. Since mmHawkeye utilizes the PMM feature of the UAV to track it, we can resist the impact of the UAV's motion and keeps a reliable tracking result.

4.4.2 The impact of the UAV's velocity. In this experiment, We evaluate the impact of the UAV's velocity on the detection performance. Due to the page limit, we only show the detection results of different UAV velocities at the altitude of 40m in Fig. 14. The detection accuracy varies slightly from 94.1% to 94.8% with the different UAV velocities. Since mmHawkeye removes velocity-related features from the obtained Doppler-Time diagram, the velocity of the UAV has little impact on the detection performance.

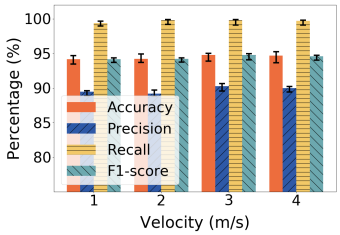

Fig. 14. The impact of UAV velocity on detection results

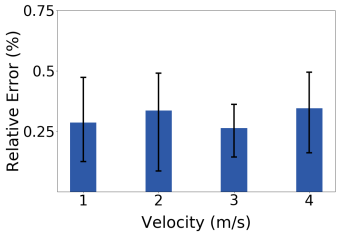

Fig. 15. The impact of UAV velocity on tracking results

We further evaluate the impact of the UAV's velocity on the tracking performance. The average relative range errors at different velocities are shown in Fig. 15. The relative range errors vary from 0.26% to 0.35% at different UAV velocities. This result demonstrates that our UAV tracking

algorithm remains effective applied under different UAV velocities. The reason is that our algorithm focuses on the frequency peaks caused by the UAV's PMM rather than the body velocity, which makes the tracking result stable even when the UAV's velocity is varied.

4.4.3 The impact of the obstacle. In this experiment, we evaluate the performance of mmHawkeye in non-line-of-sight (NLoS) scenarios. We place a large piece of obstacle of different materials 30cm above the radar to block the LoS path. The thickness of each material is about 1cm. The detection results with different obstacle materials at 40m UAV altitude are shown in Fig. 16. The detection accuracy varies slightly from 93.8% to 95.5%. This result shows that mmHawkeye remains accurate in these NLoS scenarios. It also implies that the devices deployed by mmHawkeye can be protected by enclosures of those materials, while keeping satisfactory performance. This is indeed an inspiring experience, especially when we consider the deployment of mmHawkeye in practice.

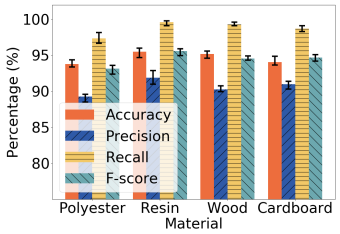

Fig. 16. The impact of obstacle material on detection results

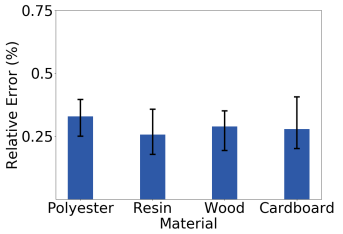

Fig. 17. The impact of obstacle material on tracking results

We also evaluate the impact of the obstacle material on the tracking performance. The average relative range errors with different obstacle materials are shown in Fig. 17. The relative range errors vary from 0.26% to 0.33% with different obstacle materials. The results again demonstrate the applicability and dependability of mmHawkeye in NLoS scenarios.

4.5 Ablation Study

As the feature extraction module in mmHawkeye serves the other two modules and cannot be evaluated separately, we conduct ablation study on UAV tracking and UAV identification modules separately. The impact of feature extraction module can be verified by comparing with the experimental results of intensity-based approach.

4.5.1 UAV tracking. This section evaluates the performance of the UAV tracking algorithm. We select the reflected signals when the UAV altitude is 40m as the target of processing. Then we respectively adopt the tracking method (1) based on the maximum value of the folding results (PMM-based), (2) based on the maximum value of the preprocessed folding results (+Prepro), (3) with dynamic programming of the preprocessed folding results (+DP), (4) with dynamic programming and particle filtering of the preprocessed folding results (+PF). The method +PF is the algorithm used in mmHawkeye.

The experiment result is shown in Fig. 18. The results demonstrate that both the preprocessing and the dynamic programming significantly reduce the range error by 16.4% and 35.12%, respectively. The reason is that the preprocessing removes the static background noise from the folding results, and the dynamic programming considers the trajectory continuity and can resist the impact of the unpredictable UAV motions. The results also demonstrate that the particle filtering can effectively reduce the variation of the range error by 13.83%, since it can effectively resist the impact of the unpredictable motions and the local dynamic noise. Furthermore, the intensity-based approach

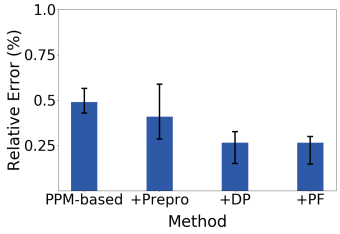

Fig. 18. Ablation study on UAV tracking

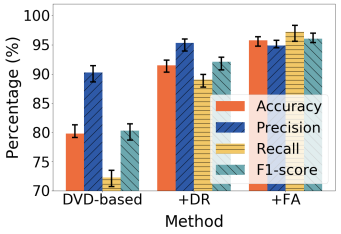

Fig. 19. Ablation study on UAV identification

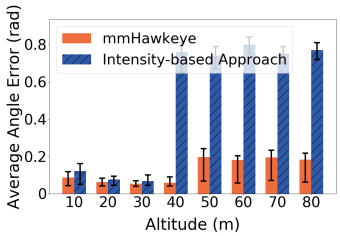

Fig. 20. The average azimuth errors

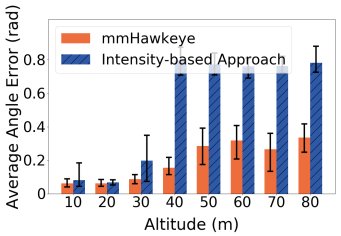

Fig. 21. The average elevation errors

fails when the UAV altitude is 40m, and our simple PMM-based method can achieve a relative range error of 0.49%. This means that spectrum folding can significantly improve UAV tracking accuracy.

4.5.2 UAV identification. This subsection evaluates the performance of the UAV identification algorithm. For the obtained Doppler-Time diagrams, we respectively perform (1) no processing (DTD-based), (2) DC removal (+DR), (3) DC removal and feature alignment (+FA) to obtain the corresponding results. The results of each method are used to train the corresponding detection network and test the detection performance. The method +FA is the algorithm used in mmHawkeye.

The detection results of these methods are shown in Fig. 19. The results demonstrate that the DC removal can significantly improve the detection accuracy by 14.62%, since it can remove a large portion of the DC noise and make the PMM features easier to be learned. The results also show that the feature alignment can effectively improve the detection accuracy by 4.68%, since it can remove the velocity-related features from the Doppler-Time diagrams and make the periodicity of the PMM feature easier to be identified.

4.6 Angle Estimation Accuracy

We evaluate the angle estimation accuracy. The average azimuth error and the average elevation error are shown in Fig. 20 and Fig. 21, respectively. They show similar results and the azimuth estimation is more accurate. We conjecture this may be due to the asymmetric layout of the radar's antennas. mmHawkeye is consistently more accurate than the intensity-based approach, especially when the UAV altitude is above 30m. The reason is that mmHawkeye can still obtain accurate range when the UAV altitude is above 30m to limit the angle estimation error, while the intensity-based approach cannot obtain the correct UAV trajectory. Though the angle estimation error of mmHawkeye also increases, it remains in a low error range. We believe such angle estimation results are useful in informing the users of the UAV's flight trajectory.

4.7 Time Consumption

We finally measure the time consumption of each module of mmHawkeye to evaluate its real-time capability in tracking and identifying a UAV. mmHawkeye uses a desktop with Intel i9-11900H as the back end to process 11.25s mmWave samples. TABLE. 1 lists the computation time of each module. It can be observed that the total time consumption is almost 19s without angle estimation. Through in-depth analysis of the algorithm flow, the Range-Doppler-FFT part currently calculates the Doppler-FFT corresponding to all Range bins (0-93m), which can be further improved based on the previous tracking result. For example, if we only calculate one-third of Doppler-FFT results, the time consumption will be reduced to one-third of the corresponding time, which is 4.32s. such an adaptive FFT operation can ensure that the processing time is less than the data collecting time, thus ensuring that mmHawkeye can provide a real-time user experience. In addition, mmHawkeye can also provide angle estimation results for UAV trajectory informing, which is 6.36s time consumption. We find that such a time consumption is mainly caused by the beamforming operation, which is nearly 5s time overhead. Considering that the angle estimation is only used to inform the users of the UAV's flight trajectory, we believe that such a computational time delay is acceptable.

Table 1. Time analysis of each component.

Processing Step	Time (s)
Range-Doppler-FFT	12.95
Spectrum Folding	4.72
UAV Tracking	1.65
Angel Estimation	6.36
UAV Identification	0.17

5 DISCUSSION

5.1 UAV Categories

As our system is based on the PMM features, all rotary-wing UAVs with such features can be detected by our system. For UAV categories that do not have rotors, such as fixed-wing UAVs, It has been reported that their periodic micro-motions also exist due to the body vibrations [22], which may make them detectable by our system. On the other hand, the size of the UAV affects the reflected signal intensity and thus the detection range. we can accurately detect it as long as it is tracked with the help of the PMM feature. However, since the flying UAV always has periodic micro-motions, its size has little effect on the detection accuracy as long as it is tracked.

On the other hand, For UAV categories that do not have rotors, such as fixed-wing UAVs, it is difficult for our system to extract the PMM feature to achieve UAV detection and tracking. [22] mentioned that the fixed-wing UAV will also produce periodic micro-motion due to the body vibration. We will further explore this problem in our future work.

5.2 Short-range Detection

When the distance between the UAV and the radar is close (e.g. below 10m), the UAV can no longer be regarded as a whole and each part may occupy a different range bin. In this case, there will be multiple PMM features in different range bins in the Range-Doppler spectrum. We can utilize these features to further track and sense the UAV. Note that probably the UAV has already been detected by mmHawkeye before it arrives in such a close range.

5.3 Limited Angle Resolution

Due to the limited number of antennas, most of COTS mmWave radar can only achieve very limited angular resolution. For example, the used TI IWR6843ISK-ODS only contains 3 Tx antennas and 4 Rx antennas. This leads to unsatisfactory performance of mmWave radars in angle estimating. Although our angle estimation algorithm based on PMM features can effectively limit the angle estimation error, the angle estimation results still need to be improved. There are some more powerful COTS radars that can be used for accurate angle estimation, such as TI MMWCAS-RF-EVM [15], which has 12 Tx antennas and 16 Rx antennas and has a much better angle resolution. However, such radars suffer from high cost, and large form factor, making them unsuitable in daily usage scenarios. Another approach is applying Synthetic Aperture Radar (SAR) technique [34] to enhance angle resolution. For example, mmFace [50] emulates a large aperture planar antenna array by moving a commodity off-the-shelf (COTS) mmWave radar along a specific trajectory in the 2D plane and achieves precise angle measurement for face authentication. But, this causes higher energy consumption.

5.4 Multi-target Detection

Multi-target detection is another interesting problem. When there are multiple UAVs simultaneously in the FoV of the radar, their trajectories are generally well separated to ensure flight safety. We can use the difference in the range and angle dimensions to distinguish them. When their trajectories occasionally coincide, their PMM features can further help us to match their respective trajectories. The trajectory crossover problem is still an open problem in mmWave sensing. Different from the trajectory recognition method that relies on trajectory continuity, our method based on the PMM feature can distinguish these trajectories from the feature space, thereby achieving accurate trajectory recognition. We leave this problem in our future work.

5.5 Practical Deployment

In practical scenarios, UAVs can intrude into personal space at height or from around. However, considering that low-altitude UAVs are easy to be detected manually or by other approaches, and these UAVs have limited viewing angles, there are very few cases of actual intrusion into personal space from low altitude. In this case, we usually deploy the radar horizontally to detect the presence of UAVs at height rather than the presence of UAVs from around.

6 RELATED WORK

6.1 UAV Detection with mmWave Radar

With the development of COTS mmWave radar and the growing concern about UAVs, there have been some works utilizing mmWave radar to track and identify small UAVs. [58] captures the UAV 3-D motion with a novel deep neural network and achieves decimeter-level tracking accuracy within 5m. It simply utilizes the reflected mmWave signal strength of the UAV as input and focuses on short-range UAV tracking based on deep learning methods, resulting in a very limited tracking range. [3] utilizes the reflected mmWave signal intensity to calculate the distance and the elevation angle between UAV and radar, realizing the UAV tracking within 10m. It further extracts the micro-Doppler signatures from the captured UAV and achieves activity classification accuracy of 95%. Different from our method that directly uses the PMM feature in the Doppler spectrum for tracking, it first uses the reflected signal strength to track the UAV and then extracts the micro-Doppler spectrum from the tracking results for activity classification. [31] employs the constant false alarm rate (CFAR) detector on the Range-Doppler spectrum and achieves a maximum detection range of about 40m. However, its performance decreases significantly when the UAV is hovering as

the Doppler feature is less significant. On the contrary, we enhance and track the PMM features brought by the periodic micro-motion rather than the single peak brought by the body motion in the Doppler spectrum, so we can achieve more robust and accurate detection results. In conclusion, none of them can achieve long-range UAV detection with the COTS mmWave radar due to the limited reflected signal intensity. To solve this problem, we directly utilize the PMM feature of the flying UAV rather than the signal intensity to achieve long-range UAV detection.

6.2 UAV Detection with Other Devices

There have been proposals to utilize sound [11, 27, 41, 44], visual information [8], and RF signals [32] to achieve passive non-cooperative UAV detection. For example, DronePrint [27] proposes to detect a drone according to its acoustic signatures. Such approaches are susceptible to the environment noise and have a limited sensing range. [8] uses cascades of boosted classifiers on the collected videos to detect the UAV and achieve distance estimation. Such video-based approaches are easily affected by illumination conditions and complex backgrounds. Matthan [32] detects the presence of UAVs by monitoring the unique characteristics of the received WiFi signal. It achieves over 80% detection accuracy within 600m range. However, it requires non-cooperative UAVs to actively send WiFi signals, which renders silent UAVs undetectable.

6.3 Active UAV Detection

Unlike passive UAV detection methods, active UAV detection methods typically require the cooperation of UAVs. They often involve emitting signals using sensors or devices to monitor for specific signatures or signals that the drone actively emits. Researchers have explored various techniques, including RFID [52], optical markers [20, 21, 23, 38], radio signal fingerprinting [32, 35, 37, 40, 47, 48, 56], etc. For example, RFHUI [52] attaches N RFID tags to a small board and exploits the measured CSI phase information to precisely track the 6-DoF pose in a 3D space. Jin, et al [21] mounted four round LED markers onto a UAV and detected them using a static camera for UAV localization. However, it can only explore varying distances in one dimension along the camera's direction. Xie, et al [48] proposed a novel UAV downlink and uplink detection method by analyzing received signals based on a UAV communication model. Furthermore, Xiao, et al [47] analyzed the UAV downlink signals and demodulated them with a known communication protocol corresponding to a particular UAV model. To tackle RF interference, many machine learning-based approaches are presented in UAV detection [7, 29, 37]. MARTINS, et al. [37] designed a Markov models-based naïve Bayes decision mechanism to distinguish signals emitted by a UAV, and then applied a neighborhood component analysis (NCA) to select the three most significant features for UAV classification.

Our previous work [54] proposed a simplified PMM feature model, which characterizes the relationship between the periodic micro-motion of the UAV and the PMM features in the reflected signal but lacks the fine-grained theoretical model of the PMM feature. We also designed a PMM-based UAV detection and ranging method. Compared with the published conference version, we first theoretically deduce the relationship between the reflected signal and the rotation velocity of the scattering point, and then deduce the mathematical representation of the PMM feature in Section 2. Inspired by our PMM-based UAV range estimation solution, we further extend our design to estimate the UAV's angle after the range estimation results are obtained in Section 3. Then we evaluate the effectiveness of the LSTM detector, the performance of mmHawkeye in non-line-of-sight (NLoS) scenarios, angle estimation accuracy, and the time consumption of each module in Section 4. More practical issues are discussed in Section 5, including UAV categories, limited angle resolution, and multi-target detection. Finally, the difference between active UAV detection works and this work is emphasized in Section 6.

7 CONCLUSION

Defending against uninvited UAVs is an increasingly important problem nowadays. This paper presents our study on non-cooperative UAV detection and identification. Our proposal named mmHawkeye is a mmWave-sensing based approach that has broad applicability and satisfactory accuracy. With the theoretical model of the PMM feature, mmHawkeye can continuously track the UAV's location containing range, azimuth angle, and altitude angle and achieve accurate UAV identification. mmHawkeye particularly tackles the problem induced by low SNR signals and achieves long-range detection. Extensive experiments with the implemented prototype demonstrate that mmHawkeye is accurate and reliable under various settings.

ACKNOWLEDGMENTS

We would like to thank the anonymous reviewers for their valuable comments and helpful suggestions. This work is supported by the National Science Fund of China under grant No. U21B2007 and Tsinghua University - Meituan Joint Institute for Digital Life.

REFERENCES

[1] Petar Andraši et al. 2017. Night-time detection of uavs using thermal infrared camera. *Transportation Research Procedia* 28 (2017), 183–190.
[2] BBC. 2020. Australian triathlete injured after drone crash. https://www.bbc.com/news/technology-26921504.
[3] Nikethan Reddy Beeram et al. 2022. Activity Classification of an Unmanned Aerial Vehicle Using Tsetlin Machine. In *IEEE ISTM*.
[4] Guillermo Bielsa et al. 2018. Indoor localization using commercial off-the-shelf 60 GHz access points. In *IEEE INFOCOM*.
[5] Igor Bisio et al. 2018. Unauthorized amateur UAV detection based on WiFi statistical fingerprint analysis. *IEEE Communications Magazine* 56, 4 (2018), 106–111.
[6] CNA. 2020. 4 arrested after drone carrying drugs spotted over Kranji Reservoir Park. https://www.channelnewsasia.com/singapore/drone-drug-trafficking-arrest-kranji-reservoir-park-655706.
[7] Martins Ezuma et al. 2019. Detection and classification of UAVs using RF fingerprints in the presence of Wi-Fi and Bluetooth interference. *IEEE Open Journal of the Communications Society* 1 (2019), 60–76.
[8] Fatih Gökçe et al. 2015. Vision-based detection and distance estimation of micro unmanned aerial vehicles. *Sensors* (2015).
[9] Unsoo Ha et al. 2020. Contactless seismocardiography via deep learning radars. In *ACM MobiCom*.
[10] Yuan He et al. 2019. Red: Rfid-based eccentricity detection for high-speed rotating machinery. *IEEE TMC* (2019).
[11] Yuan He et al. 2023. Acoustic Localization System for Precise Drone Landing. *IEEE Transactions on Mobile Computing* (2023).
[12] Sepp Hochreiter and Jürgen Schmidhuber. 1997. Long short-term memory. *Neural computation* (1997).
[13] Texas Instruments Incorporated. 2020. Real-time data-capture adapter for radar sensing evaluation module. http://www.ti.com/tool/DCA1000EVM.
[14] Texas Instruments Incorporated. 2022. Hardware Setup for MMWAVEICBOOST and IWR6843ISKODS. https://training.ti.com/hardware-setup-mmwaveicboost-and-antenna-module?keyMatch=IWR6843ISKODS.
[15] Texas Instruments Incorporated. 2022. MMWCAS-RF-EVM: mmWave cascade imaging radar RF evaluation module. https://www.ti.com/tool/MMWCAS-RF-EVM?keyMatch=MMWCAS-RF-EVM.
[16] Chengkun Jiang et al. 2019. 3D-OmniTrack: 3D tracking with COTS RFID systems. In *ACM/IEEE IPSN*.
[17] Chengkun Jiang et al. 2020. mmVib: micrometer-level vibration measurement with mmwave radar. In *ACM MobiCom*.
[18] Meng Jin et al. 2022. A Passive Eye-in-Hand" Camera" for Miniature Robots. In *ACM SenSys*.
[19] Meng Jin et al. 2023. Fast, Fine-grained, and Robust Grouping of RFIDs. In *ACM MobiCom*.
[20] Ren Jin et al. 2019. Ellipse proposal and convolutional neural network discriminant for autonomous landing marker detection. *Journal of Field Robotics* 36, 1 (2019), 6–16.
[21] Ruibing Jin and Jianliang Wang. 2016. A vision tracking system via color detection. In *2016 12th IEEE International Conference on Control and Automation (ICCA)*. IEEE, 865–870.
[22] Ki-Bong Kang et al. 2021. Analysis of micro-Doppler signatures of small UAVs based on Doppler spectrum. *IEEE TAES* (2021).
[23] Azarakhsh Keipour et al. 2021. Real-time ellipse detection for robotics applications. *IEEE Robotics and Automation Letters* 6, 4 (2021), 7009–7016.
[24] Abdelwahed Khamis et al. 2020. RFWash: a weakly supervised tracking of hand hygiene technique. In *ACM SenSys*.

[25] Md Abdullah Al Hafiz Khan et al. 2016. RAM: Radar-based activity monitor. In *IEEE INFOCOM*.
[26] Song Min Kim and Tian He. 2015. Freebee: Cross-technology communication via free side-channel. In *ACM MobiCom*.
[27] Harini Kolamunna et al. 2021. Droneprint: acoustic signatures for open-set drone detection and identification with online data. In *ACM UbiComp*.
[28] Jian Li et al. 2003. On robust Capon beamforming and diagonal loading. *IEEE TSP* (2003).
[29] Hongjie Liu. 2021. Unmanned Aerial Vehicle Detection and Identification Using Deep Learning. In *2021 International Wireless Communications and Mobile Computing (IWCMC)*. IEEE, 514–518.
[30] Yunhao Liu et al. 2010. Long-term large-scale sensing in the forest: recent advances and future directions of greenorbs. *Frontiers of Computer Science in China* (2010).
[31] Peter Joseph Basil Morris and KVS Hari. 2021. Detection and localization of unmanned aircraft systems using millimeter-wave automotive radar sensors. *IEEE Sensors Letters* (2021).
[32] Phuc Nguyen et al. 2017. Matthan: Drone presence detection by identifying physical signatures in the drone's rf communication. In *ACM MobiSys*.
[33] Wei Nie et al. 2021. UAV detection and identification based on WiFi signal and RF fingerprint. *IEEE Sensors Journal* 21, 12 (2021), 13540–13550.
[34] F. ROCCA et al. 1989. SYNTHETIC APERTURE RADAR:A NEW APPLICATION FOR WAVE EQUATION TECHNIQUES1. *Geophysical Prospecting* 37, 7 (1989), 809–830.
[35] Zhiyuan Shi et al. 2017. Detection of LSSUAV using hash fingerprint based SVDD. In *2017 IEEE International Conference on Communications (ICC)*. IEEE, 1–5.
[36] Page Six. 2020. Prince Harry and Meghan Markle call cops over drones flying over home. https://pagesix.com/2020/05/28/prince-harry-and-meghan-markle-call-cops-after-drones-fly-over-home/.
[37] Nasim Soltani et al. 2020. RF fingerprinting unmanned aerial vehicles with non-standard transmitter waveforms. *IEEE transactions on vehicular technology* 69, 12 (2020), 15518–15531.
[38] Xu Sun et al. 2021. An LED detection and recognition method based on deep learning in vehicle optical camera communication. *IEEE access* 9 (2021), 80897–80905.
[39] Yimiao Sun et al. 2022. AIM: Acoustic Inertial Measurement for Indoor Drone Localization and Tracking. In *ACM SenSys*.
[40] Yimiao Sun et al. 2023. BIFROST: Reinventing WiFi Signals Based on Dispersion Effect for Accurate Indoor Localization. In *ACM SenSys*.
[41] Yimiao Sun et al. 2023. Indoor Drone Localization and Tracking Based on Acoustic Inertial Measurement. *IEEE Transactions on Mobile Computing* (2023).
[42] Saeed V Vaseghi. 2008. *Advanced digital signal processing and noise reduction*. John Wiley & Sons.
[43] Weiguo Wang et al. 2022. MicNest: Long-Range Instant Acoustic Localization of Drones in Precise Landing. In *ACM SenSys*.
[44] Weiguo Wang et al. 2023. Acoustic Localization of Drones in Precise Landing: The Research and Practice with MicNest. *GetMobile: Mobile Computing and Communications* (2023).
[45] Wikipedia. 2022. Real-time kinematic positioning. https://en.wikipedia.org/wiki/Real-time_kinematic_positioning.
[46] Chenshu Wu et al. 2020. mmTrack: Passive multi-person localization using commodity millimeter wave radio. In *IEEE INFOCOM*.
[47] Yue Xiao and Xuejun Zhang. 2019. Micro-UAV detection and identification based on radio frequency signature. In *2019 6th international conference on systems and informatics (ICSAI)*. IEEE, 1056–1062.
[48] Yuelei Xie et al. 2021. Dual-source detection and identification system based on UAV radio frequency signal. *IEEE Transactions on instrumentation and measurement* 70 (2021), 1–15.
[49] Chenhan Xu et al. 2019. Waveear: Exploring a mmwave-based noise-resistant speech sensing for voice-user interface. In *ACM MobiSys*.
[50] Weiye Xu et al. 2022. Mask does not matter: Anti-spoofing face authentication using mmWave without on-site registration. In *ACM MobiCom*.
[51] Kun Yang et al. 2022. WiImg: Pushing the Limit of WiFi Sensing with Low Transmission Rates. In *IEEE SECON*.
[52] Jian Zhang et al. 2020. RFHUI: an RFID based human-unmanned aerial vehicle interaction system in an indoor environment. *Digital Communications and Networks* 6, 1 (2020), 14–22.
[53] Jia Zhang et al. 2022. AmbiEar: mmWave Based Voice Recognition in NLoS Scenarios. *ACM UbiComp* (2022).
[54] Jia Zhang et al. 2023. mmHawkeye: Passive UAV Detection with a COTS mmWave Radar. In *IEEE SECON*.
[55] Jia Zhang et al. 2023. A Survey of mmWave-Based Human Sensing: Technology, Platforms and Applications. *IEEE Communications Surveys & Tutorials* (2023).
[56] Caidan Zhao et al. 2017. Detection of unmanned aerial vehicle signal based on Gaussian mixture model. In *2017 12th International Conference on Computer Science and Education (ICCSE)*. IEEE, 289–293.

[57] Jie Zhao et al. 2022. Vision-based anti-uav detection and tracking. *IEEE Transactions on Intelligent Transportation Systems* 23, 12 (2022), 25323–25334.
[58] Peijun Zhao et al. 2021. 3D Motion Capture of an Unmodified Drone with Single-chip Millimeter Wave Radar. In *IEEE ICRA*.

Received July 2023; revised October 2023; accepted December 2023